Particle Orbit Theory

Jae Woo Chang
School of Mathematics and Statistics
University of St Andrews

April 2024

Abstract

This paper explores the intricate dynamics of charged particles moving in electromagnetic fields, a fundamental aspect of plasma physics. At the heart of this study is the particle orbit theory, which elucidates how charged particles gyrate, drift, and undergo acceleration under the influence of magnetic and electric fields that vary in space and time. Through analytical methods and numerical simulations, we delve into the Lorentz force equation to describe particle trajectories, emphasizing the effects of homogeneous and inhomogeneous magnetic fields, the interplay between electric fields and magnetic gradients, and the phenomena of cyclotron resonance and magnetic mirroring.

Key findings highlight how variations in magnetic field strengths alter the Larmor radius and cyclotron frequency, significantly impacting particle confinement—a principle critical to the design of magnetic confinement devices in fusion reactors. We also investigate the E×B drift, and gradient drift, providing insights into particle transport mechanisms in plasmas. Furthermore, this work examines the role of adiabatic invariants in particle motion, shedding light on the conditions under which these invariants hold and their implications for particle acceleration and trapping in natural and laboratory plasmas.

Declaration

I declare that the material submitted for assessment is my own work except where credit is explicitly given to others by citation or acknowledgement. This work was performed during the current academic year except where otherwise stated.

Acknowledgements

I am grateful to my supervisor, Thomas Neukirch, for his continuous support throughout this academic year, especially in introducing me to ideas that I was not previously familiar with, especially in the field of particle orbit theory. His insight and feedback have been greatly valued. Also, I would like to thank my family and friends for the support they have provided for my project and degree. Their unwavering belief in my abilities and their encouragement during challenging times have been a source of strength and motivation for me. Above all, I extend my deepest gratitude to my family.

Contents

Introduction

The exploration of particle orbit theory stands as a compelling gateway to the intricacies of plasma physics and moreover, applied mathematics. Initially, the endeavor to solve the equations of motion for a single charged particle in specified electric and magnetic fields might not seem the most intuitive path toward unraveling the complexities of plasmas. Plasmas, with their rich tapestry of collective interactions and the intricate interplay between currents and fields, suggest a realm far beyond the simplicity implied by individual particle trajectories. Yet, it is within this seeming simplicity that the profound depth and utility of orbit theory are revealed. This theory not only simplifies the complex dynamics of plasmas but also uncovers fundamental principles that extend across the vast expanse of plasma physics.

The allure of particle orbit theory lies in its elegant simplicity and its potent applicability across a broad spectrum of plasma phenomena. It furnishes a foundational framework that brings clarity to the understanding of plasma behaviors, from the motion of high-energy particles in the tenuous plasmas of space to the principles governing magnetic confinement in fusion devices. Through orbit theory, a unified perspective on seemingly disparate plasma phenomena is achieved, highlighting its indispensability in the field.

Embarking on a study of particle orbit theory necessitates a nuanced understanding of the conditions under which this theoretical construct remains valid. Predominantly, orbit theory is expected to excel in scenarios involving high-energy particles in low-density plasmas, where the rarity of collisions allows for a clearer examination of particle dynamics. A crucial aspect of this theory's applicability hinges on the minimal influence of self-consistent fields generated by neighboring charges, compared to the predefined external fields. This prerequisite of minimal external influence, coupled with the need for a certain degree of symmetry in the fields for analytical solutions to be feasible, delineates the scope within which orbit theory proves most effective.

A key to the success of orbit theory in describing plasma dynamics lies in the scaling introduced by an external magnetic field. The definitions of the Larmor radius and cyclotron frequency as natural length and frequency scales, respectively, facilitate the analytical resolution of the equations of motion within inhomogeneous and time-dependent fields. This methodological approach allows for an elegant separation of the rapid gyromotion from the more gradual dynamics of the guiding center, a concept that owes its origin to Alfven and remains central to our understanding of plasma behavior.

This dissertation sets out to navigate through the fundamental aspects of particle orbit theory, elucidating principles from the basic Lorentz equation to the nuanced discussions on motion in various electromagnetic field configurations. Through a detailed examination of homogeneous and inhomogeneous fields, gradient and curvature drifts, time-varying fields, and the principles of adiabatic invariance, this work aims to both consolidate and expand the existing knowledge base. In doing so, it reaffirms the pivotal role of particle orbit theory in the broader context of plasma physics, showcasing its enduring relevance and extensive applicability.

Chapter One

Particle Orbit Theory

1.1 Fundamental of particle orbit theory

The Lorentz equation forms the bedrock of particle orbit theory, serving as the fundamental equation that describes the force acting on a charged particle moving through electric (E) and magnetic (B) fields. This equation encapsulates the interplay between charged particles and electromagnetic fields, a fundamental aspect of plasma physics. Understanding this interaction is crucial for exploring the dynamics of individual particles in plasmas, thereby illuminating broader plasma behaviors and phenomena.

1.1.1 The Lorentz Force Equation

The Lorentz force equation is mathematically expressed as:

$$F = q(E + v \times B) \tag{1.1}$$

Here, $\mathbf{F}$ represents the force exerted on the particle, q is the charge of the particle, $\mathbf{E}$ is the electric field, $\mathbf{v}$ is the velocity of the particle, and $\mathbf{B}$ is the magnetic field. The cross product $\mathbf{v}\times\mathbf{B}$ highlights the velocity-dependent force that is perpendicular to both the velocity of the charged particle and the magnetic field, a distinctive characteristic that underpins the complex motion of charged particles in magnetic fields (Britannica, 2024).

Electric Force ($q\mathbf{E}$)

The electric component of the Lorentz force, $q\mathbf{E}$, describes the force exerted by an electric field $\mathbf{E}$ on a charged particle with charge q. This force is directly proportional to both the magnitude of the charge and the strength of the electric field. The electric force acts in the direction of the electric field for a positively charged particle and in the opposite direction for a negatively charged particle. This component of the Lorentz force is responsible for accelerating charged particles along the field lines of the electric field, altering their speed but not their direction of motion if the magnetic field is absent or parallel to the electric field (Britannica, 2024).

Magnetic Force ($q\mathbf{v}\times\mathbf{B}$)

The magnetic component of the Lorentz force, $q\mathbf{v}\times\mathbf{B}$, arises from the motion of a charged particle with velocity $\mathbf{v}$ through a magnetic field $\mathbf{B}$. Unlike the electric force, the magnetic force is perpendicular to both the velocity of the particle and the magnetic field direction. This results in a force that does not do work on the particle (since it acts perpendicular to the direction of motion), but instead changes the direction of the particle's velocity, leading to circular or helical trajectories. The magnitude of this force depends on the component of the velocity perpendicular to the magnetic field, and it influences the particle's motion without altering its kinetic energy (Britannica, 2024).

1.1.2 Maxwell's Equations

Maxwell's equations describe how electric and magnetic fields are generated and altered by charges and currents, and how they propagate through space. They consist of the following four equations:

Gauss's law for electricity is given by:

$$\nabla \cdot \mathbf{E} = \frac{\rho}{\epsilon_0} \tag{1.2}$$

which states that the divergence of the electric field $\mathbf{E}$ is proportional to the charge density ρ, with ϵ_0 being the vacuum permittivity (Britannica, 2024).

Gauss's law for magnetism is expressed as:

$$\nabla \cdot \mathbf{B} = 0 \tag{1.3}$$

indicating the absence of magnetic monopoles and that magnetic field lines are continuous, forming closed loops (Britannica, 2024).

Faraday's law of induction is written as:

$$\nabla \times \mathbf{E} = -\frac{\partial \mathbf{B}}{\partial t} \tag{1.4}$$

describing how a time-varying magnetic field $\mathbf{B}$ induces an electric field $\mathbf{E}$.

Ampère's law with Maxwell's addition is given by:

$$\nabla \times \mathbf{B} = \mu_0 \mathbf{J} + \mu_0 \epsilon_0 \frac{\partial \mathbf{E}}{\partial t} \tag{1.5}$$

which relates the magnetic field $\mathbf{B}$ to the electric current density $\mathbf{J}$ and the time rate of change of the electric field $\mathbf{E}$, where μ_0 is the vacuum permeability (Britannica, 2024).

The equations in the document define the current density $\mathbf{j}(\mathbf{r}, t)$ and the charge density $q(\mathbf{r}, t)$ in a plasma, which are fundamental to the interactions described by Maxwell's equations and the Lorentz force.

1. **Current Density** ($\mathbf{j}(\mathbf{r}, t)$): Defined as the sum over the product of the charge e_j and velocity $\dot{\mathbf{r}}_j(t)$ of each charged particle j within the plasma, where N is the total number of charged particles. Mathematically, it is given as:

$$\mathbf{j}(\mathbf{r}, t) = \sum_{j=1}^{N} e_j \dot{\mathbf{r}}_j(t) \delta(\mathbf{r} - \mathbf{r}_j(t)) \tag{1.6}$$

   where $\delta(\mathbf{r} - \mathbf{r}_j(t))$ is the Dirac delta function, ensuring the current density is localized at the particle positions (Boyd, 2003).

2. **Charge Density** ($q(\mathbf{r}, t)$): Similar to current density, the charge density is the sum over all particles, given by the charge of each particle e_j times the Dirac delta function, ensuring localization (Boyd, 2003):

$$q(\mathbf{r}, t) = \sum_{j=1}^{N} e_j \delta(\mathbf{r} - \mathbf{r}_j(t)) \tag{1.7}$$

1.2 Constant Homogeneous Magnetic Field

The simplest problem in orbit theory is that of the non-relativistic motion of a charged particle in a constant, spatially uniform magnetic field, $\mathbf{B}$, with $\mathbf{E} = 0$. Moreover, we shall see that it is straightforward to deal with more general cases as perturbations of this basic motion.

In a constant homogeneous magnetic field where the electric field $\mathbf{E}$ is zero, the behavior of a charged particle is influenced solely by the magnetic field $\mathbf{B}$. The force acting on a particle with charge q and velocity $\mathbf{v}$ is described by the Lorentz force, which, without an electric field, simplifies to (Gombosi, 1998):

$$\mathbf{F} = q(\mathbf{v} \times \mathbf{B}) \tag{1.8}$$

Given that $\mathbf{B}$ is uniform, the Lorentz force is perpendicular to the particle's velocity and causes the particle to move in a circular path characterized by the Larmor radius, r_L, and a cyclotron frequency, ω_c, expressed as (Gombosi, 1998):

$$r_L = \frac{mv_\perp}{|qB|}, \quad \omega_c = \frac{|qB|}{m} \tag{1.9}$$

Here, m represents the particle's mass, $v_\perp$ is the velocity component perpendicular to the magnetic field, and B is the field's magnitude .

The particle's trajectory combines uniform circular motion, due to $v_\perp$, with any linear motion resulting from a parallel component $v_{||}$, rendering the particle's path helical along the field lines (Gombosi, 1998).

The kinetic energy T of the particle is conserved:

$$T = \frac{1}{2}mv^2 = \frac{1}{2}m(v_\perp^2 + v_{||}^2) \tag{1.10}$$

Furthermore, the particle's magnetic moment μ is given by:

$$\mu = \frac{mv_\perp^2}{2B} \tag{1.11}$$

This magnetic moment is an adiabatic invariant in the context of a constant homogeneous magnetic field when $E = 0$. Adiabatic invariance indicates that if the magnetic field changes slowly in comparison to the particle's motion, the value of μ remains unchanged. This concept is pivotal in plasma physics and is leveraged in magnetic confinement fusion to achieve stable plasma conditions (Gombosi, 1998).

1.3 Constant Homogeneous Electric and Magnetic fields

1.3.1 Crossed Electric and Magnetic Fields ($\mathbf{E} \perp \mathbf{B}$)

When electric ($\mathbf{E}$) and magnetic ($\mathbf{B}$) fields are perpendicular to each other, the motion of a charged particle is characterized by:

1.3.2 $E \times B$ Drift

The drift velocity, $\mathbf{v}_d$, for all charged particles is given by:

$$\mathbf{v}_d = \frac{\mathbf{E} \times \mathbf{B}}{B^2}$$

This drift is perpendicular to both $\mathbf{E}$ and $\mathbf{B}$ fields, affecting the entire plasma uniformly without contributing to a net current (Sturrock, 1994).

1.3.3 Cyclotron Motion

Besides the drift, particles also undergo cyclotron motion around the magnetic field lines. The radius (r_L) and frequency (ω_c) of this motion are given by:

$$r_L = \frac{mv_\perp}{|q|B}, \quad \omega_c = \frac{|q|B}{m}$$

where $v_\perp$ is the component of the particle's velocity perpendicular to $\mathbf{B}$ (Sturrock, 1994).

1.4 Inhomogeneous magnetic field

In the study of charged particle dynamics, the behavior of particles in inhomogeneous magnetic and electric fields becomes significantly more complex than in the case of homogeneous fields. Inhomogeneous fields are those that change in magnitude and/or direction from one point in space to another. Understanding particle motion in such fields is critical for various applications, from designing magnetic confinement systems for fusion reactors to predicting the behavior of cosmic rays (Sturrock, 1994).

1.4.1 Electric Fields

In an inhomogeneous electric field, denoted by $\mathbf{E}(\mathbf{r})$, where $\mathbf{r}$ is the position vector, the force on a particle of charge q is given by:

$$\mathbf{F}_E = q\mathbf{E}(\mathbf{r}) \tag{1.12}$$

The electric field can vary in space, so $\mathbf{E}$ is a function of the spatial coordinates $\mathbf{r}$. The particle's acceleration, by Newton's second law, is:

$$\mathbf{a} = \frac{\mathbf{F}_E}{m} = \frac{q\mathbf{E}(\mathbf{r})}{m} \tag{1.13}$$

where m is the mass of the particle. If the electric field varies linearly with position, one might express $\mathbf{E}$ as $\mathbf{E}(\mathbf{r}) = \mathbf{E}_0 + \mathbf{G}_E \cdot \mathbf{r}$, where $\mathbf{E}_0$ is the electric field at the origin and $\mathbf{G}_E$ is the gradient of the electric field (Sturrock, 1994).

1.4.2 Magnetic Fields

In inhomogeneous magnetic fields, represented by $\mathbf{B}(\mathbf{r})$, the force on a moving charged particle is determined by the Lorentz force equation:

$$\mathbf{F}_B = q(\mathbf{v} \times \mathbf{B}(\mathbf{r})) \tag{1.14}$$

Here, $\mathbf{v}$ is the velocity of the particle. Unlike electric forces, magnetic forces do no work since they always act perpendicular to the velocity of the particle. In an inhomogeneous magnetic field, $\mathbf{B}$ varies with position, which can lead to complex trajectories (Sturrock, 1994).

One particular phenomenon that occurs in inhomogeneous magnetic fields is the grad-B drift, where a particle experiences a drift perpendicular to both the magnetic field gradient and its own velocity. The drift velocity $\mathbf{v}_d$ is given by:

$$\mathbf{v}_d = \frac{mv_\perp^2}{2qB^2}\mathbf{B} \times \nabla B \tag{1.15}$$

where $v_\perp$ is the component of the particle's velocity perpendicular to the magnetic field, B is the magnetic field magnitude, and ∇B is the gradient of the magnetic field magnitude (Sturrock, 1994).

1.4.3 Equations of Motion

The equations of motion for a particle in combined inhomogeneous electric and magnetic fields are thus governed by the total Lorentz force:

$$m\frac{d\mathbf{v}}{dt} = q\left(\mathbf{E}(\mathbf{r}) + \mathbf{v} \times \mathbf{B}(\mathbf{r})\right) \tag{1.16}$$

The solutions to these equations generally require numerical methods, especially in three-dimensional configurations where analytical solutions are not feasible. The complexity arises due to the coupling between the particle's position and velocity in both the electric and magnetic field terms, leading to non-linear motion that is sensitive to initial conditions (Sturrock, 1994).

In contexts such as plasma physics or astrophysics, where inhomogeneous fields are common, these dynamics explain phenomena such as magnetic field line reconnection, particle trapping in the magnetosphere, and the behavior of plasmas in various configurations. In fusion devices, understanding these motions is key to optimizing the containment and stability of the high-temperature plasma needed for fusion reactions (Sturrock, 1994).

1.4.4 Gradient Drift

Gradient drift arises when there is a spatial gradient in the magnetic field strength. The velocity of the gradient drift, v_G, for a particle with charge q, mass m, and perpendicular kinetic energy $W_\perp$ (related to the velocity component perpendicular to $\mathbf{B}$) is given by:

$$v_G = \frac{W_\perp}{qB^2} \left(\nabla B \times \mathbf{B} \right) \tag{1.17}$$

This drift is perpendicular to both the magnetic field gradient (∇B) and the magnetic field ($\mathbf{B}$) itself (Gombosi, 1998).

1.4.5 Curvature Drift

Curvature drift occurs due to the curvature of the magnetic field lines. For a particle with parallel kinetic energy $W_\parallel$ (related to the velocity component parallel to $\mathbf{B}$), the velocity of the curvature drift, v_C, is given by:

$$v_C = \frac{2W_\parallel}{qB^2} \left(\mathbf{R}_c \times \mathbf{B} \right) \tag{1.18}$$

where $\mathbf{R}_c$ is the radius of curvature of the magnetic field lines. This drift velocity is also perpendicular to $\mathbf{B}$, but, unlike the gradient drift, it depends on the parallel kinetic energy of the particle (Gombosi, 1998).

1.5 Time-varying Magnetic Field and Adiabatic Invariance

Previously, we've discussed magnetic fields that are not homogeneous and found that many practical situations require analysis of magnetic fields that vary over time. When considering fields where the temporal change is significant compared to spatial variation, and the field's variation in time is slow $\left(\frac{|\partial \mathbf{B}|}{|\mathbf{B}|} \ll |\Omega| \right)$, we simplify the scenario to fields that vary in time but not in space. Within these fields, can we identify conserved quantities similar to the Larmor kinetic energy W_L for motion in a uniform and static field? We aim to show that under certain circumstances, it's indeed possible to define such invariants (Boyd, 2003).

A time-dependent axial magnetic field induces an azimuthal electric field, $\mathbf{E}$, resulting in a perpendicular component of velocity, $v_\perp$, that varies over time. This leads to a variation in the perpendicular kinetic energy, given by:

$$\frac{d}{dt} \left(\frac{1}{2} m v_\perp^2 \right) = \mathbf{E} \cdot \mathbf{v}_\perp. \tag{1.19}$$

As the particle traverses a Larmor orbit, the change in its energy can be described as:

$$\delta\left(\frac{1}{2}mv_{\perp}^{2}\right) = \oint \mathbf{E}\cdot d\mathbf{r}_{\perp} = e\oint(\nabla\times\mathbf{E})\cdot d\mathbf{S}, \tag{1.20}$$

where $d\mathbf{r}_{\perp} = \mathbf{v}_{\perp}dt$ and $d\mathbf{S}$ represents the surface element enclosed by the particle's path. Employing Faraday's law of induction, this alteration in kinetic energy can be connected to the evolution of magnetic flux (Boyd, 2003):

$$\delta\left(\frac{1}{2}mv_{\perp}^{2}\right) = -e\int\frac{\partial\mathbf{B}}{\partial t}\cdot d\mathbf{S}. \tag{1.21}$$

This formalism confirms the existence of adiabatic invariants for a charged particle's motion in a time-varying magnetic field and forms the basis for further exploration in fields such as plasma physics where magnetic fields are dynamic (Boyd, 2003).

As the magnetic field varies slowly, the change in the particle's perpendicular kinetic energy, denoted as $\delta\left(\frac{1}{2}mv_{\perp}^{2}\right)$, can be approximated by the expression involving the product of the Larmor radius squared, the electric charge, the absolute value of the magnetic field $|B|$, and its time derivative $\dot{B}$ (Boyd, 2003):

$$\delta\left(\frac{1}{2}mv_{\perp}^{2}\right) \approx \pi r_{L}^{2}|e||B| = \frac{mv_{\perp}^{2}}{2}\frac{2\pi}{|\Omega|}\frac{\dot{B}}{|B|} \tag{1.22}$$

It's important to recognize that the negative sign typically associated with $\dot{B}$ disappears due to the opposite signs of the electric charge and the direction of the magnetic flux change δB. If we express the change in magnetic field strength over one orbit as δB, we can relate this to the change in the perpendicular kinetic energy δW_L through (Boyd, 2003):

$$\delta W_L = W_L\frac{\delta B}{|B|} \tag{1.23}$$

This leads to the implication that the quantity $W_L/|B|$ remains constant ($\delta(W_L/|B|) = 0$), which resonates with the concept of adiabatic invariance identified by Alfvén.

The magnetic moment μ_B, defined as the ratio of the perpendicular kinetic energy to the magnetic field strength:

$$\mu_B = \frac{W_L}{|B|} \tag{1.24}$$

is an approximate constant of the motion and is one of several adiabatic invariants in magnetic fields. In Hamiltonian dynamics, these invariants are quantities that remain nearly constant when a system's trajectory changes slowly in comparison to its periodic motion. Specifically, the action integral $\int pdq$, taken over one period of the motion and involving conjugate canonical variables p and q, is one such adiabatic invariant. The critical condition for adiabatic invariance is that the trajectory must change gradually over the time scale of the basic periodic motion. The magnetic moment μ_B is associated with Larmor precession within the magnetic field (Boyd, 2003).

We discover that a charged particle can be confined between magnetic mirrors, leading to another periodicity and thus a second adiabatic invariant. If we include curvature drifts in our analysis and consider a suitably structured magnetic field, a third invariant may emerge. This invariant corresponds to the magnetic flux enclosed by the drift orbit of the particle's guiding center, further enriching our understanding of particle motion in variable magnetic fields (Boyd, 2003).

1.5.1 Invariance of the magnetic moment in an inhomogeneous field

The magnetic moment is found to be invariant even when charged particles move through spatially inhomogeneous magnetic fields—fields where the magnetic field's derivative with respect to spatial coordinates is not uniformly zero. To illustrate this concept, consider an axially symmetric magnetic field that gradually increases with the z-coordinate, as shown in the accompanying figure (Boyd, 2003).

Analyzing the divergence of this magnetic field in cylindrical coordinates, we find that the radial component of the magnetic field, rB_r, is determined by integrating the gradient of the axial component of the magnetic field, B_z, along the z-axis:

$$rB_r = -\int_0^r \frac{\partial B_z}{\partial z} r'\, dr' \tag{1.25}$$

This integral demonstrates the connection between the radial component of the magnetic field and the spatial variation of the axial magnetic field component, highlighting the field's inhomogeneity. The constancy of the magnetic moment in such a varying field is significant, as it suggests that some properties of the charged particle's motion remain unchanged despite the complexity of the spatially varying magnetic field. This principle is particularly pertinent in scenarios such as the Earth's magnetosphere or magnetic confinement devices used for plasma physics, where magnetic fields are inherently non-uniform (Boyd, 2003).

Given that the magnetic field is relatively constant over a single Larmor orbit and the radial component B_r is significantly smaller than the axial component B_z, the approximation of B_r at the Larmor radius r_L is (Boyd, 2003):

$$B_r(r_L) \approx -\frac{r_L}{2}\frac{\partial B_z}{\partial z} \approx -\frac{r_L}{2}\frac{\partial B}{\partial z} \tag{1.26}$$

Using this approximation, the change in the parallel component of velocity $v_{||}$ for a particle in this field, based on the gradient of the magnetic field along the z-direction, allows us to express the parallel component of the force in terms of the magnetic moment μ_B (Boyd, 2003):

$$m\frac{dv_{||}}{dt} = -\frac{1}{2}|e|r_L v_\perp \frac{\partial B}{\partial z} = -\frac{W_\perp}{B}\frac{\partial B}{\partial z} = -\mu_B \frac{\partial B}{\partial z} \tag{1.27}$$

Thus, we find that the time derivative of the particle's perpendicular kinetic energy is proportional to the negative product of the magnetic moment and the rate of change of the magnetic field in space (Boyd, 2003):

$$\frac{d}{dt}\left(\frac{1}{2}mv_\perp^2\right) = -\mu_B v_{||}\frac{\partial B}{\partial z} = -\mu_B \frac{dB}{dt} \tag{1.28}$$

Bringing together the above result with equation (2.30) and considering the conservation of energy, we find that the magnetic moment's rate of change with time is zero:

$$\frac{d\mu_B}{dt} = 0 \tag{1.29}$$

This invariance of μ_B in a spatially varying magnetic field has significant implications, particularly for the physics of charged particles in magnetic confinement systems, which are extensively used in fusion research. The constancy of μ_B indicates a stable behavior of charged particles in variable magnetic fields, which is a subject for further exploration in subsequent discussions (Boyd, 2003).

1.6 Magnetic mirrors

When we consider a particle moving through the spatially non-uniform magnetic field discussed earlier, we notice its path bends towards regions where the magnetic field strength, B, is increasing. This behavior aligns with the previously established invariant ratio W/B — where W is the kinetic energy associated with the particle's motion perpendicular to the magnetic field.

As the particle ventures into a region with a stronger magnetic field, W must correspondingly increase because BB is increasing and the ratio W/B must remain constant due to energy conservation. Consequently, there could exist a certain magnetic field strength (let's call it BR) where the parallel velocity component vv becomes zero. At this juncture, the particle can no longer progress further into the region of higher magnetic field strength and is effectively reflected back. This point of reflection occurs as long as the vector product $\mathbf{v}\times\mathbf{B}$ does not equal zero, embodying the characteristics of a magnetic mirror (Saslow, 2002).

To define the pitch angle, θ, of a particle's trajectory, we use the tangent of θ in terms of the perpendicular, $v_\perp$, and parallel, $v_{||}$, components of velocity (Boyd, 2003):

$$\tan\theta = \frac{v_\perp}{v_{||}} \tag{1.30}$$

Given the magnetic moment $\mu_B = \frac{W_\perp}{B}$ is a constant, it follows that the ratio $\frac{\sin^2\theta}{B}$ is also a constant. Setting B_R as a reference magnetic field, we have (Boyd, 2003):

$$\sin\theta = \left(\frac{B}{B_R}\right)^{1/2} \tag{1.31}$$

When a particle encounters a region where the magnetic field reaches its peak value B_M before being reflected, we set $B_R = B_M$. Therefore, particles with pitch angles such that $\sin\theta > \left(\frac{B}{B_M}\right)^{1/2}$ will experience reflection before hitting the maximum field region; those with a lower $\sin\theta$ will not (Boyd, 2003).

Arranging two magnetic mirror fields as shown in Figure 2.7, particles with greater pitch angles than $\left(\frac{B}{B_M}\right)^{1/2}$ will bounce back and forth between the mirrors, creating what is known as a magnetic bottle or adiabatic mirror trap. Defining the mirror ratio, R, as the magnetic field's strength from the center of the bottle, B_0, to its maximum, B_M, we get (Boyd, 2003):

$$R = \frac{B_M}{B_0} \tag{1.32}$$

Particles will be reflected within this configuration if their initial pitch angle θ_0 meets the condition:

$$\sin\theta_0 > R^{-1/2} \tag{1.33}$$

This mechanism is critical in plasma confinement systems where the geometry and strength of the magnetic field create 'traps' that contain or lose particles based on their pitch angles, a concept essential for the study of plasma behavior in both natural and man-made magnetic fields (Boyd, 2003).

Within the confines of a magnetic bottle, the relevant particles are those within a certain solid angle σ in velocity space, illustrated in Fig. 2.8. This solid angle σ defines what is known as the loss cone. The probability of particle escape from the magnetic bottle, denoted by P, is determined by the ratio of this solid angle to 2π (Boyd, 2003):

$$P = \frac{\sigma}{2\pi} = \frac{1}{2\pi} \int_0^{\theta_0} \sin\theta \, d\theta \tag{1.34}$$

where θ_0 is the apex angle of the loss cone. When expressed in terms of the mirror ratio $R = \frac{B_M}{B_0}$, with B_M representing the magnetic field at the mirror points and B_0 the field at the center, we approximate:

$$P = 1 - \left(\frac{R-1}{R}\right)^{\frac{1}{2}} \approx \frac{1}{2R} \quad \text{for} \quad R \gg 1 \tag{1.35}$$

Thus, a larger mirror ratio indicates a reduced likelihood of particle escape, enhancing the magnetic trap's efficacy.

Magnetic mirror traps have historically been utilized for laboratory plasma containment, but their use has declined due to particle losses, shifting the focus to toroidal confinement methods. Despite this, the concept of magnetic trapping is essential to our comprehension of many naturally occurring plasmas, such as the Earth's radiation belts and the energetic particles from solar flares that circulate in closed-loop fields near active regions of the Sun. Prior to examining natural magnetic traps, we must acknowledge the existence of an additional adiabatic invariant integral to these physical processes (Saslow, 2002).

1.7 The longitudinal adiabatic invariant

The diversity of adiabatic invariants within a dynamical system is related to the various periodic behaviors it exhibits. An additional invariant is anticipated in conjunction with particle reflections within the fields of a magnetic mirror trap. This second invariant pertains to the guiding center motion of the particle and is known as the longitudinal invariant, J, defined by the integral:

$$J = \oint v_{||} \, ds \tag{1.36}$$

where ds denotes an infinitesimal element of the guiding center's path, and the integration is conducted over one complete cycle of the guiding center's trajectory (Sturrock, 1994).

The utility of the longitudinal invariant J becomes apparent in contexts where the mirror points of the magnetic field are not fixed, necessitating the treatment of the magnetic field B as a variable that changes gradually in both space and time. Defining the total parallel energy of the particle as $W = \frac{1}{2}mv_{||}^2 + \mu_B B$, we can express J as a function of the path s, the parallel velocity $v_{||}$, and time t (Sturrock, 1994):

$$J(W, s, t) = \oint_{s_1}^{s_2} \left[\frac{2}{m}(W - \mu_B B)\right]^{1/2} ds \tag{1.37}$$

This formulation underscores the significance of J in describing the longitudinal aspects of a particle's confinement within a magnetic mirror trap, a principle observed in various natural and laboratory plasma contexts.

The temporal evolution of the longitudinal invariant J can be ascertained by taking into account its partial derivatives with respect to time, W (the particle's total parallel energy), and the path s, in concert with the respective rates of change of W and s (Boyd, 2003):

$$\frac{dJ}{dt} = \left(\frac{\partial J}{\partial t}\right)_{W,s} + \left(\frac{\partial J}{\partial W}\right)_{s,t} \frac{dW}{dt} + \left(\frac{\partial J}{\partial s}\right)_{W,t} \frac{ds}{dt} \tag{1.38}$$

Substituting the expression for $J(W, s, t)$, the rate of change of J becomes:

$$\frac{dJ}{dt} = -\int_{s_1}^{s_2} \left[\frac{2}{m}(W - \mu_B B)\right]^{-1/2} \left(\mu_B \frac{\partial B}{\partial t}\right) ds \tag{1.39}$$

$$+ \left(v_{||}\mu_B \frac{\partial B}{\partial t} + \mu_B v_{||} \frac{\partial B}{\partial s}\right) \int_{s_1}^{s_2} \left[\frac{2}{m}(W - \mu_B B)\right]^{-1/2} ds \tag{1.40}$$

$$+ \left[\frac{2}{m}(W - \mu_B B)\right]^{1/2} (v_{||} - v_{||}) \int_{s_1}^{s_2} \left[\frac{2}{m}(W - \mu_B B)\right]^{-1/2} \left(\mu_B \frac{\partial B}{\partial s}\right) ds \tag{1.41}$$

This analytical framework implicates integrals involving the product of the magnetic moment μ_B, the temporal and spatial rates of change of the magnetic field, alongside the parallel component of the particle's velocity. Such an equation is central to elucidating the behavior of a particle immersed in a magnetic field that varies over time and reinforces the invariance of J under certain stipulations—fundamental for plasma confinement studies and magnetic mirror trap mechanisms (Boyd, 2003).

At the particle's turning point, marked by s_1 where the parallel component of velocity $v_{||}$ becomes zero, we examine the derivative of the longitudinal adiabatic invariant J with respect to time:

$$\frac{dJ}{dt} = -\int \left[\frac{2}{m}(W - \mu_B B)\right]^{-\frac{1}{2}} \left(\mu_B \frac{\partial B}{\partial t}\right) ds \tag{1.42}$$

Upon simplification, given that $v_{||}$ is zero, the integral reduces to:

$$\frac{dJ}{dt} = \mu_B \frac{\partial B}{\partial t} \int \frac{ds}{v_{||}} \tag{1.43}$$

Further evaluating the integral over the time domain, assuming a constant rate of magnetic field change, we get:

$$\frac{dJ}{dt} = -\mu_B \int_0^{\tau_{||}} \frac{\partial B}{\partial t} dt = -\mu_B \left[B(\tau_{||}) - B(0) - \tau_{||} \frac{\partial B}{\partial t} \right] \tag{1.44}$$

This can be approximated to the order of $(\tau_{||}/\tau_f)^2$, where $\tau_{||}$ is the transit time and τ_f is the characteristic time scale for the magnetic field changes. When τ_f is substantially greater than $\tau_{||}$, it implies:

$$\frac{dJ}{dt} \approx 0 \tag{1.45}$$

This condition reflects the slow variation of the magnetic field in comparison to the transit time, validating the near-constancy of J and reinforcing the adiabatic invariance of a particle's motion within a varying magnetic field. This principle is crucial for the effectiveness of magnetic mirror confinement and provides insight into particle behavior in evolving magnetic environments (Sturrock, 1994).

1.7.1 Mirror Traps

Mirror traps, also known as magnetic mirror machines, are a type of plasma confinement system that utilizes magnetic fields to trap charged particles. The concept is based on the magnetic mirror effect, where particles moving along magnetic field lines experience an increase in magnetic field strength along their path. This increase in field strength causes the particles to slow down and eventually reverse direction, reflecting back along the field lines, much like light reflects off a mirror (Boyd, 2003).

The trap is formed by two stronger magnetic fields, known as mirror points, located at each end of a weaker field region. The strength of the magnetic field at the mirror points, B_M, is greater than that in the central region, B_0. Charged particles spiral around the magnetic field lines and move back and forth between the regions of high magnetic field, trapped by their inability to enter areas where the field strength exceeds a certain threshold (Boyd, 2003).

The effectiveness of a mirror trap is often characterized by the mirror ratio, $R = \frac{B_M}{B_0}$. Particles with velocities that have a sufficiently large component perpendicular to the magnetic field lines will be reflected at the mirror points. The perpendicular component of the particle's velocity is necessary for the magnetic moment, a conserved quantity in the adiabatic process, to generate the required magnetic force for reflection (Boyd, 2003).

However, not all particles will be trapped. There is a region of velocity space, known as the loss cone, where particles have too large a parallel velocity component. These particles can escape the trap, leading to losses. The size of the loss cone is inversely related to the mirror ratio: a higher mirror ratio means a smaller loss cone and better confinement (Boyd, 2003).

Mirror traps have historically been of interest for fusion research as they offer a relatively simple method of magnetic confinement. They were among the first devices to demonstrate significant plasma confinement times. Despite this, their application has been limited by issues such as the difficulty in maintaining stable plasma and end losses, which have led to the development of more advanced confinement concepts like tokamaks and stellarators. Nevertheless, the principles of mirror traps still apply to natural phenomena such as the Earth's magnetosphere, where the magnetic field naturally confines charged particles from the solar wind (Boyd, 2003).

1.8 Applied field of homogeneous magnetic field

A constant, homogeneous magnetic field, characterized by a magnetic field that has the same magnitude and direction at every point in space, finds applications across various domains, from basic research to technological innovations. One prominent real-life application of such fields is in Magnetic Resonance Imaging (MRI).

1.8.1 Magnetic Resonance Imaging (MRI)

MRI is a non-invasive medical imaging technology used to investigate the anatomy and physiological processes of the body in both health and disease. MRI scanners use strong, constant, homogeneous magnetic fields, along with radio waves and field gradients, to generate detailed images of the inside of the human body (National Research Council, 1996). MRI is extensively used in hospitals and clinics for diagnosing conditions affecting various parts of the body, including the brain, spine, joints, and internal organs like the heart and liver. Its ability to produce high-resolution images of soft tissues makes it invaluable for medical diagnosis, treatment planning, and research, showcasing a practical and impactful application of constant, homogeneous magnetic fields in real life.

How It Works:

- Strong Homogeneous Magnetic Field: The primary component of an MRI machine is a large, powerful magnet that produces a strong and constant magnetic field. This homogeneous field aligns the protons, particularly those in hydrogen atoms, within the water molecules in the body (National Research Council, 1996).

- Radio Frequency (RF) Pulses: Once the protons are aligned, the MRI uses short bursts of radio waves to knock the protons out of alignment. When the RF pulse is turned off, the protons realign themselves with the magnetic field, and in doing so, they emit radio waves (National Research Council, 1996).

- Signal Detection and Image Formation: The signals emitted by the protons are detected by the MRI sensors and then converted into images by a computer. The strength and homogeneity of the magnetic field directly influence the quality and speed of image acquisition. A perfectly homogeneous magnetic field ensures that the protons precess at the same frequency, leading to clearer, more precise images (National Research Council, 1996).

Importance of Homogeneity:

The homogeneity of the magnetic field in MRI is critical for achieving high-resolution images. Even slight variations in the magnetic field can lead to artifacts and distortions in the resulting images. This is why the design and maintenance of the magnets in MRI systems, to ensure they provide as constant and homogeneous a magnetic field as possible, are of paramount importance (National Research Council, 1996).

Mathematics of MRI

In Magnetic Resonance Imaging (MRI), the generation of a constant homogeneous magnetic field, denoted as B_0, is crucial. This field, measured in teslas (T), must be spatially uniform across the imaging volume to within a few parts per million. The uniformity of B_0 ensures the precision of the alignment and precessional frequency, ω_L, of hydrogen protons in the body, as described by the Larmor equation (National Research Council, 1996):

$$\omega_L = \gamma B_0 \tag{1.46}$$

where γ represents the gyromagnetic ratio for hydrogen protons, approximately 2.675×10^8 rad/s/T.

Upon entering the MRI scanner, the protons align with the magnetic field B_0. The application of a radiofrequency (RF) pulse, resonant with the Larmor frequency $f = \frac{\omega_L}{2\pi}$, excites the protons. The RF pulse induces a flip angle θ in the net magnetization (National Research Council, 1996):

$$\theta = \gamma B_1 \Delta t \tag{1.47}$$

where B_1 is the magnetic field due to the RF pulse and Δt is its duration.

Post-RF excitation, the system returns to equilibrium via two primary relaxation processes, with time constants T_1 and T_2. The T_1 relaxation, or longitudinal relaxation, describes the return of the net magnetization vector to alignment with B_0 (National Research Council, 1996):

$$M_z(t) = M_0 \left(1 - e^{-\frac{t}{T_1}}\right) \tag{1.48}$$

The T_2 relaxation, or transverse relaxation, characterizes the decay of the net magnetization in the plane perpendicular to B_0:

$$M_{xy}(t) = M_0 e^{-\frac{t}{T_2}} \tag{1.49}$$

MR signals are spatially encoded using additional magnetic field gradients, G_x, G_y, and G_z. These gradients linearly alter the magnetic field across the patient, leading to a Larmor frequency that varies with position (National Research Council, 1996):

$$\omega(x, y, z) = \gamma(B_0 + G_x x + G_y y + G_z z) \tag{1.50}$$

These encoded signals are reconstructed into an image through a Fourier Transform, linking frequency and phase-encoded data with the spatial structure of the scanned subject. The mathematics of MRI illustrates a symphony between physics principles and advanced signal processing (National Research Council, 1996).

Chapter Two

Simulation of particle in python

2.1 Simulation for constant homogeneous magnetic field

2.1.1 Setting Up the Simulation

I started by defining the necessary physical constants for my simulation: the charge q and mass m of the particle, along with the strength B of the magnetic field. These constants are fundamental because they directly influence the Lorentz force, which dictates how the particle moves.

2.1.2 Implementing the Lorentz Force

I implemented the Lorentz force equation through the `lorentz_force` function. This function calculates the derivative of the particle's position and velocity at any point in time, based on how the magnetic field influences its motion. Given that the magnetic

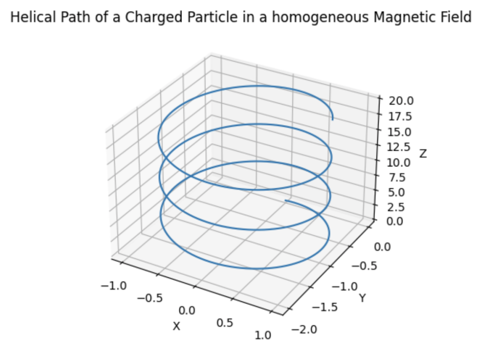

Figure 2.1: Motion of particle in constant homogeneous magnetic field

field is oriented along the z-axis, it affects the particle's velocity in the x and y directions, leading to a circular motion that is perpendicular to the direction of the field.

2.1.3 Setting Initial Conditions

For the initial conditions, I chose the particle's starting position and velocity to ensure it would exhibit a helical trajectory. By starting the particle at the origin and giving it initial velocities in the x and z directions, I could observe how it spirals along the direction of the magnetic field while also circling around it.

2.1.4 Numerically Solving the Motion

To find the particle's path over time, I used the `solve_ivp` function from SciPy's integrate module, applying it to the differential equation derived from the Lorentz force. By solving this equation across a defined time span with the specified initial conditions, I could trace the particle's position and velocity at various moments, illustrating its motion through space.

2.1.5 Visualizing the Results

For visualization, I employed Matplotlib to create a 3D plot showcasing the particle's helical path. The `plot` function enabled me to draw this path, emphasizing the combined effects of the particle's initial velocity and the magnetic field. To further illustrate the magnetic field's presence and direction, I generated a quiver plot overlaying vectors on the particle's path. These vectors, pointing along the z-axis, were plotted at regular intervals to represent the uniform magnetic field guiding the particle's motion.

2.1.6 Enhancing the Plot

I added axis labels and a title to my plot to clarify what was being shown and included a legend to distinguish between the particle's path and the magnetic field vectors. Adjusting the visual parameters of the quiver plot ensured that the magnetic field's direction was clearly communicated without detracting from the main focus on the particle's trajectory.

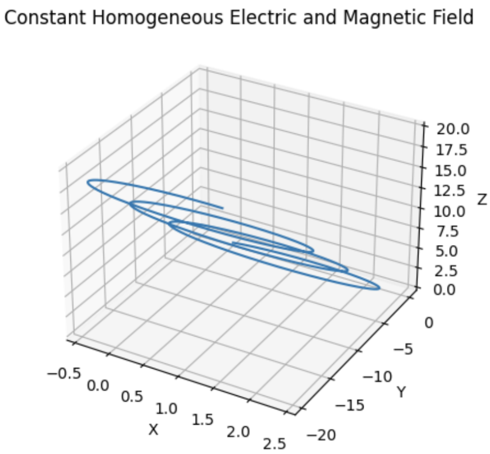

Figure 2.2: Motion of particle in constand homogeneous electric and magnetic fields

2.2 Simulation of constant homogeneous electric and magnetic field

In the enhancement of my simulation of a charged particle's motion, I introduced an electric field component to the existing model of motion in a magnetic field. This addition allows for a more comprehensive examination of the Lorentz force and its effects on the particle's trajectory.

2.2.1 Modification to the Lorentz Force Equation

The original model accounted for the magnetic field's influence on the particle, which led to a helical motion. To this model, I added the effect of a constant, homogeneous electric field, resulting in the following modified Lorentz force equation:

The addition of the electric field introduces a force component in the direction of the electric field, regardless of the particle's velocity. This is expressed in the modified differential equation as:

$$\frac{dv_x}{dt} = \frac{q}{m}(E + v_y B),$$
$$\frac{dv_y}{dt} = -\frac{q}{m}(v_x B),$$
$$\frac{dv_z}{dt} = 0.$$

2.2.2 Simulation Adjustments

The electric field strength, E, is set to 1.0, mirroring the simplicity of the magnetic field setup. The initial conditions and the time span for the simulation remained unchanged to facilitate a direct comparison between the motion induced solely by the magnetic field and the combined fields.

2.2.3 Theoretical Background

The $\mathbf{E} \times \mathbf{B}$ drift arises when a charged particle is subjected to orthogonal electric ($\mathbf{E}$) and magnetic ($\mathbf{B}$) fields. The drift velocity, $\mathbf{v}_d$, is given by:

$$\mathbf{v}_d = \frac{\mathbf{E} \times \mathbf{B}}{B^2},$$

where $\mathbf{v}_d$ is the drift velocity, $\mathbf{E}$ is the electric field, $\mathbf{B}$ is the magnetic field, and B is the magnitude of the magnetic field.

2.2.4 Simulation Setup

In the simulation, the electric field is applied along the x-axis ($\mathbf{E} = E_0\hat{x}$), and the magnetic field is aligned along the z-axis ($\mathbf{B} = B_0\hat{z}$). This configuration leads to a drift movement in the y-direction, perpendicular to both $\mathbf{E}$ and $\mathbf{B}$.

2.2.5 Observation of ExB Drift

Due to the Lorentz force, the particle experiences a force that causes it to move in a direction perpendicular to both fields. This results in a uniform drift across the electric and magnetic fields, observable in the simulation as a motion perpendicular to the initial plane defined by the electric and magnetic fields. Specifically, with $\mathbf{E}$ along the x-axis and $\mathbf{B}$ along the z-axis, the drift velocity $\mathbf{v}_d$ occurs along the y-axis, demonstrating the cross-field drift effect. The simulation provides a clear visualization of the $\mathbf{E} \times \mathbf{B}$ drift phenomenon, showcasing how charged particles move in a direction perpendicular to both applied electric and magnetic fields. This drift is a fundamental concept in magnetized plasmas and plays a significant role in various physical processes and devices, such as magnetic confinement in fusion reactors and the behavior of the ionosphere.

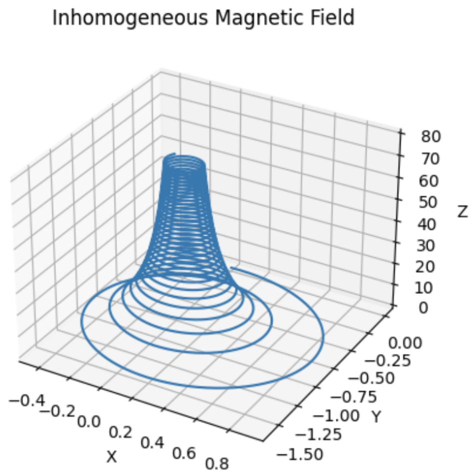

Figure 2.3: Motion of particle in Inhomogeneous magnetic field

2.3 Simulation of inhomogeneous magnetic field

In a simulation exploring the dynamics of a charged particle moving in an inhomogeneous magnetic field, where the magnetic field strength increases linearly with height in the z-direction ($B = B_0 + \alpha z$), two key phenomena are observed: changes in the Larmor radius and alterations in the cyclotron frequency. As the particle ascends through regions of increasing magnetic field strength, its Larmor radius, r_L, decreases due to the inverse relationship between r_L and B ($r_L \propto \frac{1}{B}$). Mathematically, this is expressed as:

$$r_L = \frac{mv_\perp}{qB}$$

where m is the particle's mass, $v_\perp$ is the velocity component perpendicular to the magnetic field, and q is the charge of the particle. Simultaneously, the cyclotron frequency, ω_c, which dictates the rate of the particle's gyration around magnetic field lines, increases with the magnetic field strength ($\omega_c \propto B$). The cyclotron frequency is given by:

$$\omega_c = \frac{qB}{m}$$

This demonstrates that as the particle moves to regions with higher z values, encountering stronger magnetic fields, it experiences a tightening spiral path characterized by a smaller Larmor radius and completes rotations around the magnetic field lines more rapidly due to a higher cyclotron frequency.

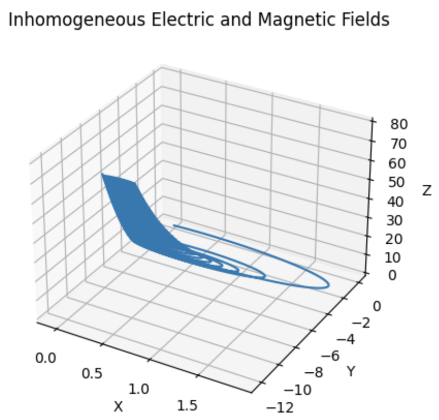

Figure 2.4: Motion of particle in inhomogeneous electric and magnetic fields

2.4 Simulation of inhomogeneous electric and magnetic fields

In this simulation, we explore the dynamics of a charged particle under the influence of both inhomogeneous electric and magnetic fields. This scenario allows for the investigation of more complex particle behaviors than those observed in homogeneous field environments.

2.4.1 Defining the Inhomogeneous Electric Field

The electric field (E) is designed to vary linearly with the z-coordinate, paralleling the previously established inhomogeneous magnetic field (B). The electric field is defined as:

$$E = E_0 + \beta z,$$

where E_0 represents the initial electric field strength at $z = 0$, and β is the constant rate at which the electric field strength increases along the z-axis.

2.4.2 Modification to the Lorentz Force Equation

To incorporate the effects of the inhomogeneous fields, the Lorentz force equation was modified within the `lorentz_force_inhomogeneous_fields` function. This modification

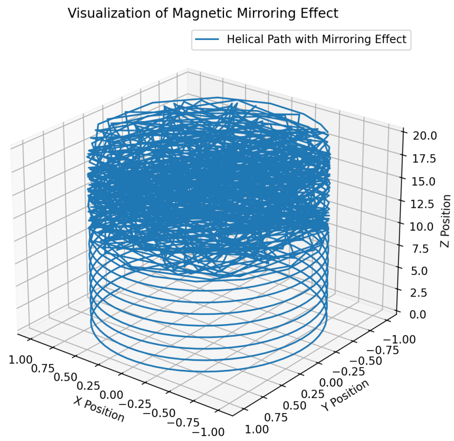

Figure 2.5: Motion of particle when Magnetic mirroring happens

integrates the linearly increasing electric field into the force calculation:

$$\frac{dv_x}{dt} = \frac{q}{m}(E + v_y B),$$
$$\frac{dv_y}{dt} = -\frac{q}{m}(v_x B),$$
$$\frac{dv_z}{dt} = 0.$$

In this model, both E and B are functions of z, highlighting their inhomogeneous nature. The dynamics of the particle's motion in the x and y directions are governed by the combined influences of the electric and magnetic fields, while its velocity in the z-direction remains unaffected by these fields.

2.5 Magnetic mirroring

This figure outlines the modifications made to a previous simulation setup to observe the magnetic mirroring effect on a charged particle moving in an inhomogeneous magnetic field.

2.5.1 Adjusting Magnetic Field Inhomogeneity

I increased the rate at which the magnetic field strength increases with the z-coordinate by setting the coefficient α to 0.5. This change creates a more pronounced gradient in the magnetic field strength along the z-axis, which is essential for observing the magnetic mirroring effect. In magnetic mirroring, particles spiral along magnetic field lines and reflect or "mirror" back at points where the magnetic field strength significantly increases.

2.5.2 Eliminating the Electric Field

I removed the influence of the electric field by setting the initial electric field strength (E_0) to 0 and ensuring it does not vary with z ($\beta = 0$). This decision focuses the simulation purely on the effects of the magnetic field, as magnetic mirroring is a phenomenon that can be observed without the complicating factor of an electric field.

2.5.3 Modifying Initial Conditions

To effectively demonstrate magnetic mirroring, I adjusted the initial conditions to give the particle a higher velocity in the z-direction ($v_z = 5$), positioning it closer to regions of higher magnetic field strength. This adjustment ensures that the particle reaches the area where the magnetic field gradient is sufficient to cause mirroring.

2.5.4 Solving the Differential Equation

With these adjustments, I solved the Lorentz force differential equation using the same numerical method but under the new conditions. This approach calculates the particle's trajectory, demonstrating how it spirals along the magnetic field lines and undergoes reflection at points where the magnetic field strength significantly increases.

Conclusion

In conclusion, this dissertation has traversed the complex terrain of particle orbit theory, providing a comprehensive examination of charged particle dynamics in electromagnetic fields. From the foundational principles governing the behavior of particles in both homogeneous and inhomogeneous magnetic fields to the nuanced understanding of drift motions and adiabatic invariants, this work has laid bare the intricate mechanisms that underpin particle motion in plasma environments.

The exploration of particles in homogeneous magnetic fields revealed how the Larmor radius and cyclotron frequency serve as critical parameters in determining particle trajectories, offering essential insights into the principles of magnetic confinement. This theoretical foundation was further enriched by delving into the complexities of particles navigating through inhomogeneous magnetic fields, highlighting the significant roles of gradient, curvature, and drifts in particle transport processes.

Through the lens of applied mathematics, this dissertation showcased the profound impact of particle orbit theory on the development and optimization of Magnetic Resonance Imaging (MRI) technology. The simulations conducted not only illustrated the practical implications of controlled particle motion within magnetic fields but also underscored the theory's critical contribution to enhancing MRI's diagnostic capabilities. By manipulating magnetic fields to influence particle orbits, MRI technology leverages these principles to produce high-resolution images of internal body structures, demonstrating the theory's tangible benefits in medical diagnostics.

Moreover, the simulations presented in this work have illuminated the dynamic behavior of particles under various electromagnetic conditions, offering visual and quantitative evidence of the theoretical concepts discussed. These simulations not only serve as a bridge between theory and application but also provide a valuable tool for predicting and analyzing particle dynamics in a range of plasma environments.

Bibliography

Boyd, T.J.M. and Sanderson, J.J. (2003) *The Physics of Plasmas*. Cambridge: Cambridge University Press. (Accessed: [10, Oct 2023])

National Research Council (US) and Institute of Medicine (US) Committee on the Mathematics and Physics of Emerging Dynamic Biomedical Imaging. (1996). Washington (DC): National Academies Press (US). Available at: http://www.nap.edu/ (Accessed: [31, Jan 2024]).

Saslow, W, M. (2002). How Electric Currents Interact with Magnetic Fields. Magnetic Mirror. (Accessed: [31, Jan 2024])

Sturrock, P.A. (ed.) (1994) 'Orbit theory', in *Plasma Physics: An Introduction to the Theory of Astrophysical, Geophysical and Laboratory Plasmas*. Cambridge: Cambridge University Press, pp. 19-31, pp. 49–65. (Accessed: [24, Feb 2024])

Gombosi, T.I. (1998) 'Particle Orbit Theory', in *Physics of the Space Environment*. Cambridge: Cambridge University Press (Cambridge Atmospheric and Space Science Series), pp. 3–29. (Accessed: [12, March 2024])

Britannica, T. Editors of Encyclopaedia (2024). Lorentz force. Encyclopedia Britannica. https://www.britannica.com/science/Lorentz-force (Accessed: [12, March 2024])

Britannica, T. Editors of Encyclopaedia (2024). Maxwell's equations. Encyclopedia Britannica. https://www.britannica.com/science/Maxwells-equations (Accessed: [12, March 2024])

Reference for python simulating: https://flothesof.github.io/charged-particle-trajectories-

E-and-B-fields.html